Global Change Biology

Global Change Biology (2012) **18**, 371–384, doi: 10.1111/j.1365-2486.2011.02546.x

TECHNICAL ADVANCE

The Dual Arrhenius and Michaelis–Menten kinetics model for decomposition of soil organic matter at hourly to seasonal time scales

ERIC A. DAVIDSON*, SUDEEP SAMANTA*, SAMANTHA S. CARAMORI† and KATHLEEN SAVAGE*

*The Woods Hole Research Center, 149 Woods Hole Road Falmouth, MA 02540-1644, USA, †Unidade de Ciências Exatas e Tecnológicas, The Universidade Estadual de Goiás, Rodovia BR 153 Km 98, CEP: 75132-903, Anápolis, Goiás, Brazil

Abstract

Decomposition of soil carbon stocks is one of the largest potential biotic feedbacks to climate change. Models of decomposition of soil organic matter and of soil respiration rely on empirical functions that relate variation in temperature and soil water content to rates of microbial metabolism using soil-C substrates. Here, we describe a unifying modeling framework to combine the effects of temperature, soil water content, and soluble substrate supply on decomposition of soluble soil-C substrates using simple functions based on process concepts. The model's backbone is the Michaelis–Menten equation, which describes the relationship between reaction velocity and soluble organic-C and O_2 substrate concentrations at an enzyme's reactive site, which are determined by diffusivity functions based on soil water content. Temperature sensitivity is simulated by allowing the maximum velocity of the reaction (V_{max}) to vary according to Arrhenius function. The Dual Arrhenius and Michaelis–Menten kinetics (DAMM) model core was able to predict effectively observations from of laboratory enzyme assays of β-glucosidase and phenol-oxidase across a range of substrate concentrations and incubation temperatures. The model also functioned as well or better than purely empirical models for simulating hourly and seasonal soil respiration data from a trenched plot in a deciduous forest at the Harvard Forest, in northeastern United States. The DAMM model demonstrates that enzymatic processes can be intrinsically temperature sensitive, but environmental constrains of substrate supply under soil moisture extremes can prevent that response to temperature from being observed. We discuss how DAMM could serve as a core module that is informed by other modules regarding microbial dynamics and supply of soluble-C substrates from plant inputs and from desorption of physically stabilized soil-C pools. Most importantly, it presents a way forward from purely empirical representation of temperature and moisture responses and integrates temperature-sensitive enzymatic processes with constraints of substrate supply.

Keywords: climate change, CO_2, soil carbon, soil respiration, Q_{10}

Received 21 June 2011 and accepted 27 July 2011

Introduction

The large magnitudes of soil carbon stocks and fluxes loom large in global carbon budgets and in consideration of climate change feedbacks (Davidson & Janssens, 2006; Tarnocai *et al.*, 2009; Bond-Lamberty & Thomson, 2010). Models of decomposition of soil organic matter and of soil respiration rely heavily on empirical functions that relate variation in temperature and soil water content to rates of microbial metabolism using soil-C substrates. This often includes various forms of fitted Q_{10} or Arrhenius functions for temperature sensitivity (Lloyd & Taylor, 1994; Sierra, 2011) and polynomial, parabolic, or other functions for sensitivity to variation in soil moisture (Davidson *et al.*, 2000). Skopp *et al.* (1990) described a conceptual model of aerobic heterotrophic respiration in soils that encompassed soluble carbon limitation in dry soils, oxygen limitation in wet soils, and optimal conditions for respiration at intermediate water contents. Most efforts to incorporate these ideas in models have used only empirical fits using a variety of polynomial and parabolic equations (Linn & Doran, 1984; Doran *et al.*, 1991; Davidson *et al.*, 2000). Moreover, the parameters of these functions have little or no mechanistic or biophysical meaning, and the parameterization of these temperature and moisture functions tends to be site specific, which impedes the development of robust models that are broadly applicable. Indeed, debate remains in the literature concerning the temperature sensitivity of decomposition of soil organic matter (Davidson & Janssens, 2006; von Lützow

Correspondence: Eric A. Davidson, tel. + 1 508 444 1832, fax + 1 508 444 1532, e-mail: edavidson@whrc.org

& Kögel-Knabner, 2009; Kirschbaum, 2010; Sierra, 2011), because observations of apparent temperature sensitivity vary widely among studies and among seasons within study sites. The potential for confounding effects of temperature, moisture, and substrate supply to obscure the effects of any one of these drivers alone has been well recognized (Ryan & Law, 2005; Davidson *et al.*, 2006a; Subke & Bahn, 2010), but a solution to that problem remains elusive.

A large part of the discussion about effects of temperature on decomposition of soil organic matter centers around chemical and physical protection of organic substrates on mineral surfaces and within soil aggregates (Davidson & Janssens, 2006). We do not address that topic here, other than to show how the model that we present focusing on soluble substrates and extracellular enzymes could eventually be linked to these other processes of C stabilization and destabilization in soils. Instead, we focus here on rapidly cycling soil-C substrates, which either are soluble or become soluble once soluble extracellular enzymes react with them. Depolymerization of organic-C compounds by extracellular enzymes has been proposed as the rate-limiting step for heterotrophic respiration in soils and for fast-response decomposition (Bengtson & Bengtsson, 2007). Hence, our focus is on how substrate supply, as affected by diffusion in liquid and gas phases in the soil, interacts with temperature-dependent enzymatic processes to produce CO_2. These interactions have been shown to potentially affect apparent temperature sensitivity of CO_2 production (Davidson *et al.*, 2006a). We seek to use the principles of Michaelis–Menten and Arrhenius kinetics to describe these interactions.

Here, we describe a relatively simple model based on process concepts that uses seven linked equations to combine the effects of temperature, soil water content, and soluble substrate supply on decomposition of soil-C substrates in a unifying modeling framework (Fig. 1). The backbone of the model is the Michaelis–Menten equation, which describes the relationship between reaction velocity and soluble organic-C and O_2 substrate concentrations at the reactive site of an enzyme. Temperature sensitivity is represented in the model by allowing the maximum velocity of the reaction (V_{max}) to vary according to an Arrhenius function. The model structure also permits the half-saturation constants (*kM*s, also referred to as the Michaelis constants) to be temperature sensitive in a way that counteracts some or all of the V_{max} induced temperature sensitivity of the reaction velocity (Davidson *et al.*, 2006a). Furthermore, we explore how substrate limitation can also dampen the expression of temperature sensitivity of V_{max} regardless of whether *kMs* are also temperature sensitive.

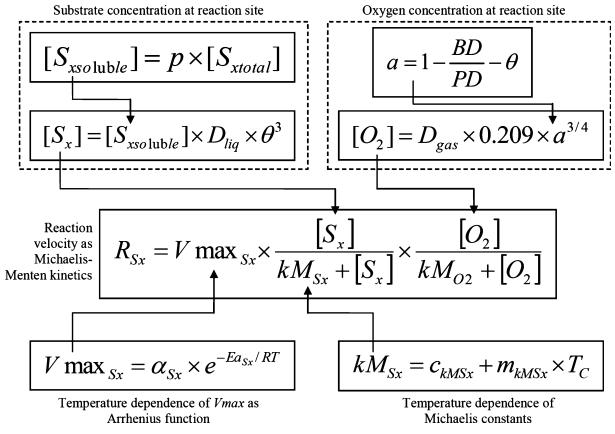

Fig. 1 A graphical representation of the compartmentalized structure of the DAMM model.

The concentrations of both soluble organic-C and O_2 at the simulated reaction site are determined by diffusivity functions, which, in turn, are simulated as functions of soil water content. The parameters of the Arrhenius, Michaelis–Menten, and diffusivity equations must still be calibrated to observed responses for accurate simulation of a specific system, but the mathematical functions representing the interactions of temperature, water content, and substrate supply are based on a mechanistic understanding of these interactions. Hence, the calibrated parameter values can be interpreted in physical terms relatively more easily compared to those obtained by fitting a polynomial function. This also facilitates the identification of reasonable parameter values for the model for an application where no data are available for direct calibration. Moreover, as the processes are simulated as separate functional components in this modeling framework, advancements in the understanding of these processes, such as seasonal dynamics of substrate supply in the soil, can be integrated into the model.

We test the adequacy of the model structure for simulating soil respiration using data from both laboratory and field experiments. Laboratory assays of two enzymes commonly found in soils were used to explore the adequacy of the model structure under controlled conditions and to assess the number of parameters needed to represent these processes. Data from a field trenching experiment at the Harvard Forest were then used to challenge the model with seasonal and diel variation in measured soil respiration *in situ*, where the potentially confounding effect of variation in root respiration had been experimentally excluded. We use this modeling framework to demonstrate how the apparent temperature sensitivity of the reaction velocity is dependent not only on the prescribed activation energy

of the Arrhenius function, but also on the supply and diffusion of substrates, which depend largely on soil water content. We postulate that much of the variability of temperature sensitivity of soil respiration reported in the literature could be explained by this modeling framework. Moreover, we discuss how this simple model could interface with more complex models of substrate availability and supply, diffusion, and microbial dynamics in the soil.

Materials and methods

Model description

The backbone of the Dual Arrhenius and Michaelis–Menten (DAMM) kinetics model is a Michaelis–Menten equation [Eqn (1); Fig. 1] for two substrates, soluble carbon (S_x) and oxygen (O_2). For the moment, we use S_x to refer to all soluble substrates, but it could be differentiated into any number of substrates (S_1, S_2, S_3, etc.) to represent specific compounds (e.g. glucose, tannin) or families of compounds (e.g. simple sugars, amino acids, polyphenols). Including O_2 as a substrate defines the scope to aerobic respiration, which is the dominant form in most upland soils, but the model could be modified to include anaerobic processes by substituting different electron acceptors in place of O_2. The reaction velocity, R_{S_x}, is calculated in the model as:

$$R_{S_x} = V_{\max_{S_x}} \times \frac{[S_x]}{kM_{S_x} + [S_x]} \times \frac{[O_2]}{kM_{O_2} + [O_2]}, \quad (1)$$

where $V_{\max_{S_x}}$ is the maximum velocity of the enzymatic reaction, when substrate concentrations are not limiting, $[S_x]$ and $[O_2]$ are concentrations of S_x and O_2, respectively, and kM_{S_x} and kM_{O_2} *are* the corresponding Michaelis constants. $V_{\max_{S_x}}$ is calculated according to an Arrhenius function:

$$V_{\max_{S_x}} = \alpha_{S_x} \times e^{-Ea_{S_x}/RT}, \quad (2)$$

where R is the universal gas constant, T is the temperature in Kelvin, α_{S_x} and Ea_{S_x} are the pre-exponential factor and activation energy of the enzymatic reaction with S_x, respectively. This model structure assures that, providing substrate concentrations are not limiting, the respiration rate is sensitive to temperature according to Arrhenius kinetics.

We experimented with the alternatives that the Michaelis constants are sensitive to temperature or that they are constants with respect to temperature. The temperature sensitivity of kM_{S_x} was modeled using a simple linear function:

$$kM_{S_x} = c_{kM_{S_x}} + m_{kM_{S_x}} \times T_C, \quad (3)$$

where T_C is the temperature in Celsius, $c_{kM_{S_x}}$ and $m_{kM_{S_x}}$ are the intercept and slope parameters, respectively. We consider the linear form of Eqn (3) to be a null model 'place-holder' that could be replaced by a different function if it is supported by emerging theory or empirical evidence. However, we are unaware of any first-principles justification for either linear or nonlinear relationships between Michaelis constant and temperature. The few data that exist on temperature effects on Michaelis constant can be fit parsimoniously with linear functions (S. Allison, personal communication; Berry & Raison, 1981; Lonhienne *et al.*, 2001; Hochachka & Somero, 2002), but they do not rule out other functions. Similarly, we presently consider kM_{O_2} to be constant with respect to temperature, however, kM_{O_2} could also be modeled as a function of temperature, if data were available to support it.

An abbreviated version of the DAMM model, using only Eqns (1)–(3) is used with the data described below from laboratory enzyme analyses, where it is assumed that neither O_2 availability nor diffusion of substrates is limiting. For use with field data, however, we add Eqns (4)–(7) to simulate the effects of diffusion of soluble-C and O_2 substrates.

The concentration of soluble carbon substrates at the reactive site of the enzyme ($[S_x]$) is affected by soil water content, and specifically by diffusion of substrates through soil water films. Using these underlying principles, $[S_x]$ is calculated in two steps in the DAMM model. In the first step, we make a simplifying assumption that the amount of the substrate S_x in soluble form ($[S_{x\text{soluble}}]$) is a constant fraction of the total carbon content:

$$[S_{x\text{soluble}}] = p \times [S_{x\text{total}}], \quad (4)$$

where $[S_{x\text{total}}]$ is the total amount of the substrate S_x in the bulk soil, in both soluble and insoluble forms, and p is the fraction of $[S_{x\text{total}}]$ that is soluble. As discussed below, other model modules may be developed to focus on the fraction of total soil-C that becomes soluble by various mechanisms, but that is beyond the scope of the current effort. In the second step, $[S_x]$ is calculated from $[S_{x\text{soluble}}]$ as:

$$[S_x] = [S_{x\text{soluble}}] \times D_{\text{liq}} \times \theta^3, \quad (5)$$

where θ is the volumetric water content of the soil, and D_{liq} is a diffusion coefficient of the substrate in liquid phase (Papendick & Campbell, 1981). For simplicity, we use a dimensionless diffusion coefficient which differs from the traditional diffusivity coefficient used in Fick's law, which typically have units of volume over distance and time. We make this simplification for two reasons: (i) we discuss later how more complex model structures might simulate two- or three-dimensional heterogeneity or use probability density functions to represent distributions of diffusion distances, but that is beyond the scope of this initial modeling effort; and (ii) creating a dynamic model that is resolved in discrete time steps is also a longer term goal, but would add computational demands that might obscure our present purpose of presenting a basic model structure. We selected values for p and D_{liq} [Eqns (4) and (5)] based on prior experimental observations on Harvard Forest soils as discussed further in the Field data. Diffusion of soluble substrates has been shown to be related to the thickness of the soil water films, which is approximated by the cube of the volumetric water content (Papendick & Campbell, 1981). In reality, extracellular enzymes may also diffuse to substrates in addition to substrates diffusing to the enzymes, but both should follow similar functions of water film thickness. While we explicitly represent the diffusion of soluble carbon substrate, $[S_x]$, to the enzyme reaction site in

Eqn (5), this equation effectively simulates the combined effect of both substrate and enzyme diffusion. In any case, the concentration of the substrate at the reactive site of the enzyme declines with declining soil water content, thus rendering the kM_{S_x} factor increasingly important in Eqn (1) as water content declines.

The concentration of O_2 at the reactive site of the enzyme depends upon diffusion of gases within the soil medium, which is represented in the model according to a simple function of air-filled porosity (Millington, 1959; Eqn (6)). In the model, $[O_2]$ is calculated as:

$$[O_2] = D_{gas} \times 0.209 \times a^{4/3}, \quad (6)$$

where D_{gas} is a diffusion coefficient for O_2 in air, 0.209 is the volume fraction of O_2 in air, and a is the air-filled porosity of the soil. Following the same reasoning described above for our approach for defining D_{liq}, we use a dimensionless D_{gas} that differs from that traditionally used in Fick's law. The total porosity is calculated from bulk density (BD) and particle density (PD). Air-filled porosity, a, is calculated by subtracting volumetric water content (θ) from total porosity (Davidson & Trumbore, 1995) as:

$$a = 1 - \frac{BD}{PD} - \theta. \quad (7)$$

As water content increases, a declines and $[O_2]$ at the reaction site of the enzyme declines as a power function of a. Hence, the kM_{O_2} term in Eqn (1) becomes increasingly important as θ increases.

The interactions of these equations are illustrated in Fig. 1. In summary, these seven equations merge Michaelis–Menten kinetics of potentially substrate-limited enzymatic reactions with temperature-dependent Arrhenius kinetics of $V_{max_{S_x}}$ for nonsubstrate limited conditions, taking into consideration the physical processes of how soil water content affects diffusion of the soluble-C and O_2 substrates. Each of the equations is based on process-level understanding of enzyme kinetics and physical processes of diffusion, except for the two equations describing the effects of temperature on Michaelis constants, for which little theory exists and a simple empirical relationship is provisionally employed with testing against data from our own laboratory experiments (see below under 'Enzyme analyses').

The complete DAMM model is tested against field data (see below under 'Field data') and in comparison to two empirical models developed for similar data from the same site (Savage *et al.*, 2009). One is a purely Q_{10} function defined by:

$$R = R_{ref} \times Q^{\left(\frac{T_S - 10}{10}\right)}, \quad (8)$$

and the other is a Q_{10} and water content function defined by:

$$R = R_{ref} \times D^{(M_{opt} - M)^2} \times Q^{\left(\frac{T_S - 10}{10}\right)}, \quad (9)$$

where R represents respiration, R_{ref} is the reference R (mg C m^{-2} h^{-1}) at 10 °C, Q is the Q_{10} parameter that represents the change in R with a 10 °C change in temperature, T_S is half hourly soil temperature 10 cm depth (°C), M is the soil moisture (cm^3 H_2O cm^{-3} soil in %) from 2 to 8 cm, and M_{opt} is the optimum soil moisture which is set at the maximum % soil moisture content encountered in the data and D is a calibrated parameter. All models were fitted using nonlinear least squares approach using the nls function in the statistical package R, version 2.12.2 (R Development Core Team, 2011). For model fitting, the parameter α_{S_x} [Eqn (2)] was transformed to $\ln(\alpha_{S_x})$ to avoid convergence problems.

To facilitate refinement of this model and linkages to proposed modules suggested in the discussion section, the version of the DAMM model used in this analysis is made available in the form of R functions in the linked supplemental material on the journal web site (see Appendix S1).

Enzyme analyses

We utilized the enzyme analyses data primarily to test the core [Eqns (1) and (2)] of the model. An additional goal was to evaluate whether the temperature dependence for kM_{S_x} [Eqn (3)] improves the model, as opposed to a using a constant value. The third term on the right hand side of Eqn (1) was not used, as O_2 was not limiting for these assays. For the constant kM_{S_x} model, kM_{S_x} (μmol L^{-1}) was calibrated directly, but for temperature-dependent kM_{S_x} model, $c_{kM_{S_x}}$ (μmol L^{-1}) and $m_{kM_{S_x}}$ (μmol L^{-1} $°C^{-1}$) were calibrated instead. The parameters α_{S_x} (μmol h^{-1} g^{-1} soil) and Ea_{S_x} (kJ mol^{-1}) were calibrated in both cases.

Organic and mineral A horizon soil samples were collected from the Harvard Forest (see section below on Field data). Triplicate samples were composited, passed through a 2 mm sieve, and stored at 4 °C and at field moisture. Water content was determined by drying subsamples at 105 °C so that results can be converted to a dry-weight basis. Soil extracts were prepared following Šnajdr *et al.* (2008), with some modifications. Briefly, 1.0 g dry-mass equivalent of soil was added to 0.25 mL toluene and either 4.0 mL (β-glucosidase assay) or 40 mL (phenol-oxidase assay) of 100 mM phosphate buffer. This extract was agitated on an orbital shaker for 60 min and centrifuged at 8000*g* and 20 °C. The supernatant was retained for enzyme assays. All assays were carried out in triplicate aliquots on acrylic microplates, using a Power Wave XS2 plate reader (Biotek Instruments Inc., Winooski, VT, USA). The microplates were incubated at 4, 12, 20, 27, or 37 °C. Activity of β-glucosidase was measured following Valásková *et al.* (2007) utilizing *p*-nitrophenyl-β-D-glucoside (PNG) as substrate at six concentrations ranging from 0.62 to 80 mmol L^{-1}. The reaction was stopped after 60 or 120 min by adding 0.1 mL of 0.5 M sodium carbonate, and absorbance was read at 400 nm. The activity of phenol-oxidase was measured following Saiya-Cork *et al.* (2002), using L-3,4-dihydroxyphenylalanine (L-DOPA) as substrate at concentrations from 0.12 to 15 mmol L^{-1}. Absorbance was measured at 450 nm after incubation in the dark for 7 h for mineral soil extracts and 10 h for organic soil extracts. Reaction velocity was calculated using an extinction coefficient determined using horseradish peroxidase.

Field data

We challenge the DAMM model with field data of soil respiration to test whether its mechanistic structure can perform as

well or better than traditional empirical functions of temperature and moisture content. Soil respiration was measured at the Harvard Forest near Petersham, Massachusetts USA (42°32N, 72°11W), at the 'Little Prospect Hill' study site, which supports a mixed hardwood forest (dominant species *Quercus rubra* and *Acer rubrum*), approximately 60 years old and 16–20 m height. Soils are well drained and classified as Canton fine sandy loam, Typic Distrochrepts. The mean annual temperature is +7.9 °C and the mean annual precipitation is 1100 mm.

On 6 November 2008, a trench was dug to 1 m depth around a 5 × 5 m area, which severed all roots leading into the trenched plot. Plastic tarp was placed along the walls of the trench and then backfilled. Three automated soil respiration chambers were placed in each of the trenched and untrenched plots. This site has little understory vegetation, but what was present in the treatment plot was clipped on 29 May 2009. Automated measurements of soil respiration (Savage & Davidson, 2003; Savage *et al*., 2008) were made once per half hour for each chamber. Pretrenching flux measurements for all six chambers were made in 2008, and posttrenching measurements were made from 22 April through 31 October 2009. Here, we utilize only data from the trenched plot, which represent the heterotrophic component of soil respiration. Volumetric soil moisture was measured at 8–16 cm depth every 15 min using Campbell Scientific Water Content Reflectometer (Campbell Scientific, North Logan, UT) (CS616) probes. Data were aggregated to half hourly intervals to correspond to respiration measurement rates. Soil temperature was measured (type T-thermocouple) at 10 cm depth at half hourly intervals.

The trenching experiment was not replicated, due to the prohibitive costs of building and maintaining a large number of automated soil respiration chambers. Replication would be necessary if our objective were to make quantitative estimates that are meant to be representative mean values for the entire forest. Instead, the objective of the trenching experiment was to measure temporal patterns, which tend to be similar among plots within the forest despite differences in plot means for any single time point (Davidson *et al*., 1998; Savage & Davidson, 2001). A still more modest objective for the present modeling paper is to challenge the model with field data from a single plot without roots to explore whether this new model structure based on kinetics and diffusivity functions can represent the temporal variation of heterotrophic respiration as well as empirical functions of temperature and moisture content.

Explicit representation of processes requires DAMM to use a larger number of parameters, as compared to purely empirical models. However, calibrating all the parameters simultaneously is not feasible for this study due to limited information content in the calibration data and strong interactions among parameters. Prescribing realistic values for the parameters that cannot easily be calibrated imposes useful constraints on the model based on prior knowledge of the field site. Moreover, the parameters for physical properties of the soil, such as bulk density, particle density, and diffusion coefficients, are unlikely to change temporally for simulated time periods. With the above considerations, the parameters that are not calibrated are given fixed values as follows. The parameters BD (0.80 g cm^{-3}), PD (2.52 g cm^{-3}), and $[S_{x\text{total}}]$ (0.048 g C cm^{-3} soil in the top 10 cm mineral soil) are based on published data (Gaudinski *et al*., 2000). The value of p (4.14×10^{-4}) is based on the above $[S_{x\text{total}}]$ value and the reported $[S_{x\text{soluble}}]$ mean value of 20 mg C L^{-1} bulk soil solution (i.e. 2×10^{-5} g C cm^{-3} soil) for Harvard forest mineral soils (Magill *et al*., 2000). The value of D_{liq} (3.17) is determined by assuming the boundary condition that $[S_x] = [S_{x\text{soluble}}]$ for saturated soil, i.e. all of the soluble substrate is available at the reaction site under this condition. The value used for D_{gas} (1.67) is based on another assumed boundary condition that $[O_2]$ in perfectly dry soil is the same as that in free air. The value used for kM_{O_2} (0.121 cm^3 O_2 cm^{-3} air) is the value of $[O_2]$ according to Eqn (6) at the mean value of soil moisture (0.229 cm^3 H_2O cm^{-3} soil) in 2009 at this site. The parameters α_{S_x} (mg C cm^{-3} soil h^{-1}), Ea_{S_x} (kJ mol^{-1}) and kM_{S_x} (g C cm^{-3} soil) are calibrated. With the above units, DAMM calculates soil respiration rates per unit volume of soil (mg C cm^{-3} soil h^{-1}) but the observed data are soil respiration rates per unit area of soil surface (mg C m^{-2} h^{-1}); for conversion, an effective soil depth of 10 cm is assumed for this analysis, which is the depth from which most of the CO_2 production occurs in this soil (Davidson *et al*., 2006b). This effective soil depth is a simple multiplying factor and expected to affect only the calibrated value of α_{S_x}. For proper comparison, the DAMM model, the Q_{10} function [Eqn (8)] and the Q_{10} and water content function [Eqn (9)], which have been used previously at this site (Savage *et al*., 2009), are calibrated to the same observed soil respiration from the trenched plot using soil temperature at 10 cm depth and soil moisture between 2 and 8 cm depth as covariates following the same nonlinear least square method.

Results

Modeling data from laboratory experiments

The results of fitting the DAMM model to the enzyme analyses data, with and without temperature-dependent kM_{S_x} function, are summarized in Table 1. The difference in AIC between the two kM_{S_x} models is less than two for three out of the four enzyme–soil combinations, with the constant kM_{S_x} model having the lower AIC value. Such small differences are not significant (Burnham & Anderson, 2002), and therefore, do not support the selection of the more complex temperature-dependent kM_{S_x} function over the simpler constant kM_{S_x} function. Although, the AIC difference is significant (>10) in favor of temperature-dependent kM_{S_x} for phenol-oxidase and mineral soil combination, residual standard errors and R^2 values are comparable between the two kM_{S_x} functions. Parameter estimates and corresponding P-values for the two kM_{S_x} functions are reported in Table 2. The parameters α_{S_x}, Ea_{S_x}, and the

Table 1 Comparison of goodness of fit between temperature-dependent kM_{S_x} and constant kM_{S_x} models based on enzyme analyses data. Degrees of freedom on the residual standard errors are shown within parenthesis

	Temperature-dependent kM_{S_x}			Constant kM_{S_x}		
Data	Adjusted R^2	AIC	Residual std. error	Adjusted R^2	AIC	Residual std. error
β-glucosidase, organic soil	0.77	388.5	0.41 (356)	0.77	386.6	0.41 (357)
β-glucosidase, mineral soil	0.82	262.2	0.35 (356)	0.82	260.3	0.34 (357)
Phenol-oxidase, organic soil	0.89	582.2	0.54 (356)	0.89	581.4	0.54 (357)
Phenol-oxidase, mineral soil	0.88	790.8	0.72 (356)	0.88	800.2	0.73 (357)

Table 2 Parameter estimates and associated *P*-values for temperature dependent and constant kM_{S_x} model configurations used for enzyme analyses data. The α_{S_x} values shown here are transformed from calibrated $\ln(\alpha_{S_x})$ values, while the corresponding *P*-values are those for $\ln(\alpha_{S_x})$

		Temperature-dependent kM_{S_x}		Constant kM_{S_x}	
Data	Parameter*	Estimate	*P*-value	Estimate	*P*-value
β-glucosidase, organic soil	α_{S_x}	1.92×10^{11}	$P < 0.001$	2.94×10^{11}	$P < 0.001$
	Ea_{S_x}	64.35	$P < 0.001$	65.44	$P < 0.001$
	$c_{kM_{S_x}}/kM_{S_x}$	1.92	$P > 0.1$	1.40	$P < 0.001$
	$m_{kM_{S_x}}$	−0.02	$P > 0.1$	na	na
β-glucosidase, mineral soil	α_{S_x}	2.43×10^{10}	$P < 0.001$	2.93×10^{10}	$P < 0.001$
	Ea_{S_x}	59.19	$P < 0.001$	59.67	$P < 0.001$
	$c_{kM_{S_x}}/kM_{S_x}$	1.36	$0.05 < P < 0.1$	1.16	$P < 0.001$
	$m_{kM_{S_x}}$	−0.01	$P > 0.1$	na	na
Phenol-oxidase, organic soil	α_{S_x}	2.19×10^{6}	$P < 0.001$	1.24×10^{6}	$P < 0.001$
	Ea_{S_x}	32.76	$P < 0.001$	31.33	$P < 0.001$
	$c_{kM_{S_x}}/kM_{S_x}$	0.95	$P < 0.001$	1.26	$P < 0.001$
	$m_{kM_{S_x}}$	0.01	$P > 0.1$	na	na
Phenol-oxidase, mineral soil	α_{S_x}	2.68×10^{6}	$P < 0.001$	1.96×10^{5}	$P < 0.001$
	Ea_{S_x}	32.29	$P < 0.001$	25.76	$P < 0.001$
	$c_{kM_{S_x}}/kM_{S_x}$	0.35	$0.05 < P < 0.1$	1.86	$P < 0.001$
	$m_{kM_{S_x}}$	0.06	$P < 0.001$	na	na

*Units: α_{S_x} in μmol h^{-1} g^{-1} soil, Ea_{S_x} in kJ mol^{-1}, $c_{kM_{S_x}}$ and kM_{S_x} in mmol L^{-1}, $m_{kM_{S_x}}$ in mmol L^{-1} °C^{-1}.

kM_{S_x} parameter (where used as a constant) are highly significant ($P < 0.001$) in all cases. With the temperature-dependent kM_{S_x} model, the *P*-values for $c_{kM_{S_x}}$ and $m_{kM_{S_x}}$ vary considerably depending on the data, although, $m_{kM_{S_x}}$ is generally of very low significance compared to $c_{kM_{S_x}}$.

Plots of observations vs. predictions obtained using the constant kM_{S_x} model (Fig. 2) generally show good correspondence between observed and predicted values, although the residuals show some evidence of heteroscedasticity. Some evidence of systematic errors may be noted, which are further discussed in the discussion section. Although not shown here, the predictions obtained with the temperature-dependent kM_{S_x} function also have very similar relationships to the observations, and the residual structures do not differ substantially between the two kM_{S_x} functions.

Modeling data from field experiments

As the enzyme analyses dataset does not clearly favor the use of temperature-dependent kM_{S_x} function over constant kM_{S_x}, the more parsimonious version without temperature dependence of Michaelis constants is used for modeling the field experiment data for the results presented here. Goodness of fit statistics and estimated parameter values for DAMM, Q_{10} and water content function, and Q_{10} function models are shown in Table 3. The *P*-value is <0.001 for all model parameters. Using AIC as the criterion, the models may be ranked

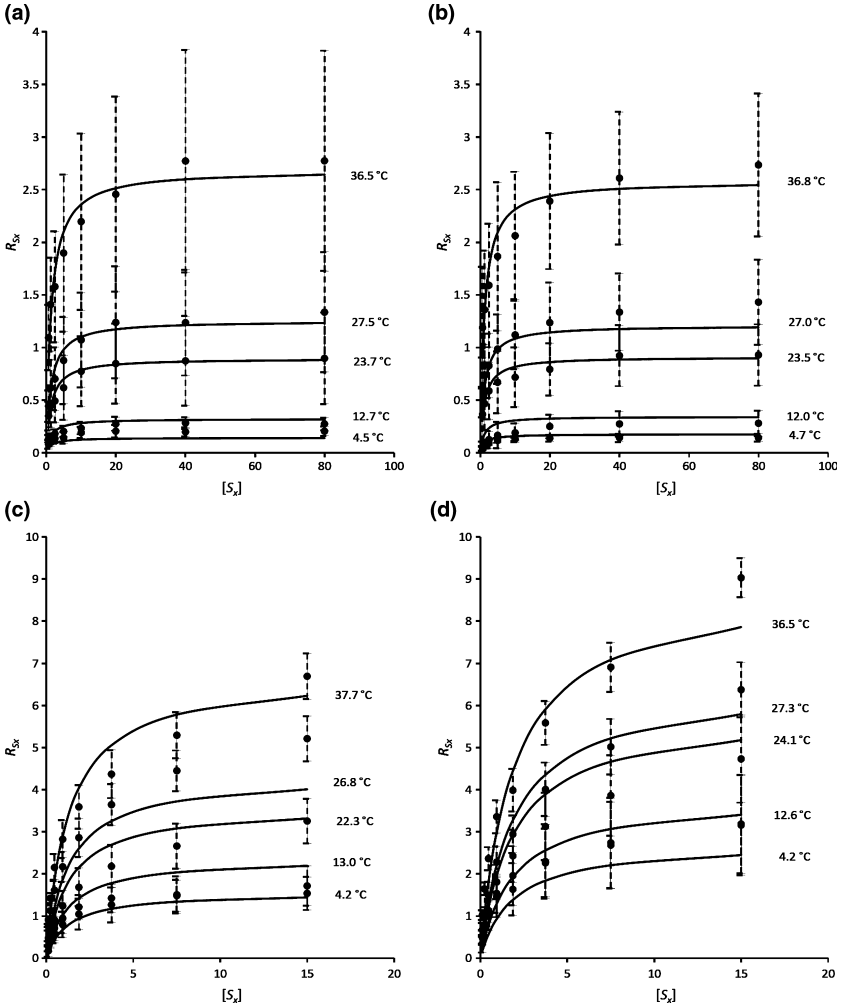

Fig. 2 Plots of predicted values (dark line) and observed mean values (points with error bars) of reaction velocity, R_{S_x} (μmol h^{-1} g^{-1} soil), for (a) β-glucosidase and organic soil, (b) β-glucosidase and mineral soil, (c) phenol-oxidase and organic soil, and (d) phenol-oxidase and mineral soil, against substrate concentration $[S_x]$ (mmol L^{-1}). The temperature (°C) corresponding to each curve is indicated by its side. The mean value and error bar (±1 SD) for each point are based on nine samples. Note that (a) and (b) use one set of scales for the axes, while (c) and (d) use a different scale.

as DAMM (AIC = 52 945), Q_{10} and water content function model (AIC = 52 951), and the Q_{10} function model (AIC = 53 212), in the order of decreasing support in the data. The difference between the first two is moderately significant, while the difference between Q_{10} function model and the other two (>260) is highly significant (Burnham & Anderson, 2002). The R^2 values for DAMM (0.50) and Q_{10} and water content function model (0.50) are also very close, while the same for the Q_{10} function (0.48) is a little lower. A visual comparison shows that the predictions have similar relationship with the observations (Fig. 3), with a slope slightly larger than one (1.03) and a small negative intercept for each model. Predicted soil respiration from DAMM is compared in further detail with the observations by plotting against the day of year (DOY) (Fig. 4), which shows that the predictions approximately match the dynamics of the observations, i.e. increasing or decreasing along with the observations. The full range of variability in soil respiration across soil temperature and soil moisture is not fully captured by the model; however, most of the extreme residual values correspond to only 1 day of year (DOY 199). The predictions also do not show any consistent trend of over or under estimation across the range of soil temperature or soil moisture (plots not shown).

Seasonal variation

Microbial biomass, enzyme production, and thermal acclimation can vary seasonally, leading to different relationships between soil respiration and soil tempera-

Table 3 Estimates of goodness of fit and parameter values for DAMM, Q_{10} and water content function, and Q_{10} function models based on 2009 field data. Uncertainties equivalent to 1 SE are shown in parenthesis with the estimated parameter values

	Parameter estimate
DAMM (R^2 = 0.50, AIC = 52 945)	
α_{S_x} ($mgCcm^{-3}soilh^{-1}$)	5.38×10^{10} (3.47×10^{10}, 8.34×10^{10})
Ea_{S_x} ($kJmol^{-1}$)	72.26 (71.22, 73.30)
kM_{S_x} ($gCcm^{-3}soil$)	9.95×10^{-7} (8.77×10^{-7}, 1.11×10^{-6})
Q_{10} and water content function (R^2 = 0.50, AIC = 52 951)	
R_{ref} ($mgCm^{-2}h^{-1}$)	69.59 (67.55, 71.63)
Q (dimensionless)	2.84 (2.80, 2.88)
D (dimensionless)	0.995 (0.992, 0.998)
Q_{10} function (R^2 = 0.48, AIC = 53 212)	
R_{ref} ($mgCm^{-2}h^{-1}$)	54.04 (53.54, 54.55)
Q (dimensionless)	2.90 (2.86, 2.95)

ture and moisture in different seasons (Bradford *et al.*, 2010). Such seasonal effects are not explicitly included in the structure of DAMM, and therefore, calibrating the model parameters to the entire annual dataset might be expected to lead to systematic seasonal errors if the seasonal variations in these properties of soil microbes and enzymes are substantial. However, the DAMM model structure includes parameters that could be related to these types of variation. Therefore, the importance of accounting for seasonally variable processes may be evaluated in terms of improvement in model fit that results from allowing model parameters to vary seasonally. For example, the pre-exponent factor (a_{S_x}) in the Arrhenius function for $V_{max_{S_x}}$ [Eqn (2)] could be considered as a proxy for either microbial biomass or the quantity of extracellular enzymes. The activation energy (Ea_{S_x} in Eqn (2)) and the Michaelis constant (kM_{S_x} in Eqn (1)) could vary seasonally if the microbial community acclimates to seasonal variation in temperature by producing isoenzymes with varying activation energies or affinities for the substrate. To explore this possibility, we divided the field data into four seasons (viz., early spring from 23 April to 26 May, spring/summer from 27 May to 30 July, summer/early autumn from 31 July to 18 September, and autumn from 19 September to 30 October) and allowed one out of a_{S_x}, Ea_{S_x}, and kM_{S_x} to assume a different value in each season, while the others were held constant at its value determined based on all of the data given in Table 3.

Considerable decreases in the residual standard error and large reductions in AIC are obtained when any one of a_{S_x}, Ea_{S_x}, and kM_{S_x} is allowed to vary seasonally, relative to those obtained with all the parameters fixed at constant values (Table 4). This result identifies the strategy of using seasonally variable parameters to be significantly more effective for modeling the field data. The improvement obtained by varying a_{S_x} is nearly the same as that obtained by varying Ea_{S_x}, while that for kM_{S_x} is relatively lower. In Fig. 4, the predictions from the model with seasonally variable a_{S_x} are superimposed on those obtained with fixed annual parameters. Comparing the two predictions visually shows that the correspondence between predictions and observations could be improved and the issue of seasonal bias, particularly during spring/summer, could be addressed effectively through the use of seasonally variable parameter.

Discussion

Modeling of laboratory enzyme data

The results presented above show that the DAMM model core [Eqns (1) and (2)] is able to predict the observations from enzyme analyses very effectively. However, a few cases of systematic deviation of the predictions from the observations are also noted. For example, the model seems to have a tendency to overestimate at low substrate concentrations and to underestimate at high substrate concentrations. This problem could possibly have been remedied by extending the added substrate concentration range to a higher value, which would have been useful to better constrain the fit of $V_{max_{S_x}}$ [Eqns (1) and (2)]. As an aside, it is worth noting that most enzyme assay methods do not call for using such high maximum concentrations, which means that reported values of enzyme activity may not be the maximum potential of extant enzymes. Another example of systematic deviations is that, for all substrate concentration values of phenol-oxidase in organic soil, the predictions underestimate the observations at 26.8 °C and overestimate at 22.3 °C. A simple method for obtaining a better fit would be to calibrate $V_{max_{S_x}}$ and kM_{S_x} at each temperature independently. However, doing this might lead to a loss in general applicability of the model as the calibrated parameter values would correspond to the observed temperature values. In case such a model has to be applied at a temperature other than those observed, $V_{max_{S_x}}$ and kM_{S_x} values for that temperature would have to be obtained through extrapolation or interpolation using a function that is not explicitly incorporated in the model. As our ultimate goal is to develop a model that would apply to a wide

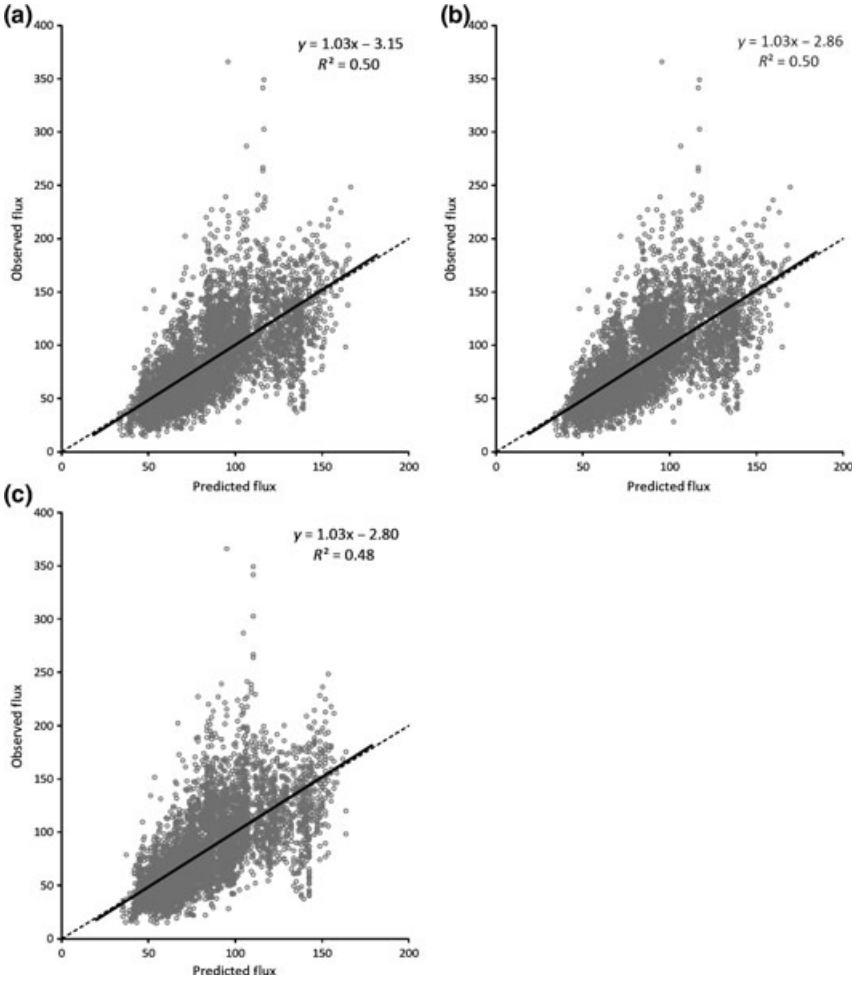

Fig. 3 Plots of predicted vs. observed soil carbon flux (mg C m^{-2} h^{-1}) for (a) DAMM, (b) Q_{10} and water content function, and (c) Q_{10} function models. Results of linear regressions between observations and predictions (continuous line) and 1 : 1 lines (dotted line) are shown on the plots for comparative evaluation.

range of conditions, rather than obtaining the best possible fit for a given set of observations, we explicitly model the temperature dependence of $V_{\max_{S_x}}$ and kM_{S_x} with respect to the entire dataset.

Modeling of field data

The comparison with the two empirically based models shows the mechanistically based DAMM is at least as credible as a purely empirical model [Eqn (9)] for the data from the field experiments. The results also indicate the need for modeling the dependence of soil respiration on soil moisture, as both models that account for this relationship perform significantly better than the Q_{10} function [Eqn (8)]. While the predicted responses surfaces for all three models, particularly those for DAMM and Q_{10} and water content function, are similar over the encountered soil temperature and moisture range, they differ markedly when the range of prediction is extended beyond the encountered range (Fig. 5). More data are needed from a wetter site to challenge the model's ability to simulate O_2 limitation. The DAMM model produces a response surface that is consistent with the empirical and conceptual models of Linn & Doran (1984) and Skopp *et al.* (1990), with peak aerobic respiration rates at intermediate water content and decreasing to lowest rates at both wet and dry extremes (Fig. 5b).

Mechanistic expressions of temperature and moisture responses

An intermediate soil moisture optimum (Linn & Doran, 1984) is obtained in the DAMM model not by assuming a polynomial or parabolic curve, but rather as a conse-

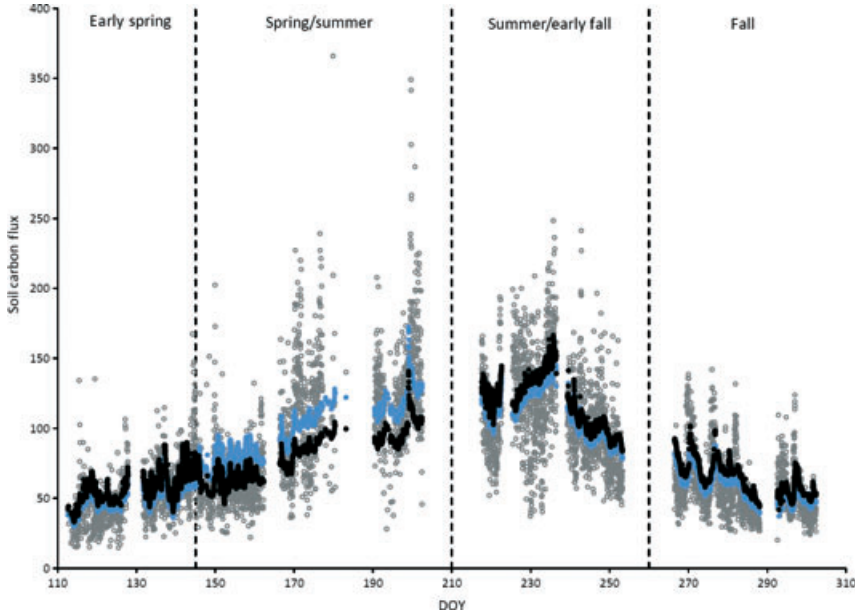

Fig. 4 Predicted soil carbon flux (mg C m^{-2} h^{-1}) from DAMM with the parameters α_{S_x}, Ea_{S_x}, and kM_{S_x} calibrated as constants for all of 2009 data (black points) and the predictions obtained by allowing α_{S_x} to have different values for different seasons (blue points) superimposed on observed values (gray points).

Table 4 Parameter estimates and AIC values obtained by allowing one of the parameters to vary by season at a time

		Parameter varied by season			
Parameter	Season	None	α_{S_x}	Ea_{S_x}	kM_{S_x}
α_{S_x}	Early spring	5.38×10^{10}	4.84×10^{10}	5.38×10^{10}	5.38×10^{10}
	Spring/summer		6.59×10^{10}		
	Summer/early autumn		5.03×10^{10}		
	Autumn		4.80×10^{10}		
Ea_{S_x}	Early spring	72.26	72.26	72.68	72.26
	Spring/summer			71.95	
	Summer/early autumn			72.59	
	Autumn			72.70	
kM_{S_x}	Early spring	9.95×10^{-7}	9.95×10^{-7}	9.95×10^{-7}	1.31×10^{-6}
	Spring/summer				7.86×10^{-7}
	Summer/early autumn				1.26×10^{-6}
	Autumn				1.36×10^{-6}
AIC		52 945	51 939	51 941	51 973
Residual standard error (degrees of freedom)		28.27 (5557)	25.82 (5556)	25.83 (5556)	25.90 (5556)

quence of modeling diffusion of soluble-C and O_2 substrates in liquid and gas phases as physically based functions of varying soil water content. While the parameters of some of these functions still need to be fit empirically for different soil types, the model and its parameters have biophysical and mechanistic meanings.

The model also demonstrates how apparent temperature sensitivity is affected by substrate limitation. The temperature sensitivity is prescribed by including an activation energy for $V_{\max_{S_x}}$ [Eqn (2)], which is fitted for the entire measurement period. However, because substrates can be limiting near low and high soil moisture extremes, the reaction rate in Eqn (1) is

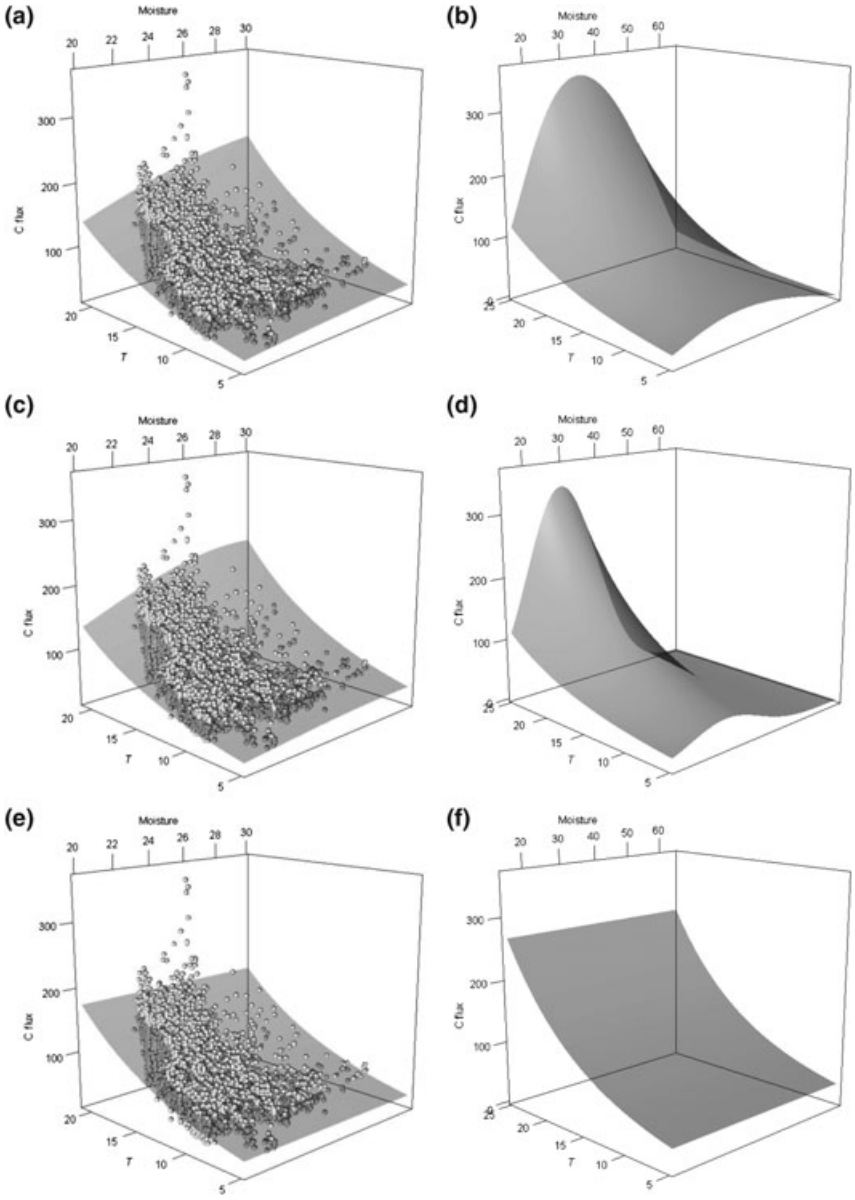

Fig. 5 Plots of predicted response surfaces for soil carbon flux (C Flux, mg C m^{-2} h^{-1}) over the range of soil temperature (T, °C) and soil moisture (moisture, % by volume) encountered in 2009 for (a) DAMM, (c) Q_{10} and water content function, and (e) Q_{10} function models, while the figures (b), (d), and (f) show the corresponding response surfaces over a wider range. The spheres in figures (a), (c), and (e) represent observations for the year 2009 (darker spheres are below the response surface).

affected not only by $V_{\max_{S_x}}$, but also by substrate concentrations. Therefore, substrate limitation can prevent the temperature effect on $V_{\max_{S_x}}$ from being fully expressed in the reaction rate. It is important to emphasize that it is not the activation energy (Ea_{S_x}) itself that is varying as a consequence of soil moisture in the DAMM model. Rather, soil moisture has no effect on Ea_{S_x} in this model structure, but it can constrict the influence of Ea_{S_x} on the overall reaction rate via its effect on substrate supply. Hence, enzymatic processes can be intrinsically temperature sensitive, as prescribed by the Arrhenius function, but environmental constrains of substrate supply can prevent that response to temperature from being observed.

In the present formulation, we used constant kM_{S_x} values, because our laboratory studies did not justify adding an additional parameter to account for temperature dependence of kM_{S_x}. However, others have reported a positive correlation between temperature and kM_{S_x} of

several enzymes (Hochachka & Somero, 2002). If that were the case, then the reaction rate would be become even less temperature sensitive at low substrate concentrations, because the temperature sensitivity of kM_{S_x} would counteract that of $V_{\max_{S_x}}$ (Davidson *et al.*, 2006a).

Linking the DAMM model structure to other soil processes

The DAMM model is conceived as representing a module of a larger model, potentially constructed of other modules representing other processes in belowground C cycling. In its current form, DAMM simulates substrate limitation at the active site of enzymatic reactions only as a consequence of diffusional constraints. For simplicity, the supply of soluble-C is not dynamic and is assumed to be a fraction of a much larger total C pool [Eqns (4) and (5)], which, for the time periods simulated here, renders it nearly inexhaustible, which is obviously unrealistic. Although our focus here is on soluble-C and the release of soluble-C due to activity of soluble extracellular enzymes, this model could be integrated with other modules that simulate the mechanisms of release of C substrates from stabilized forms, such as aggregate formation and destruction and sorption/desorption from mineral surfaces (Conant *et al.*, 2011). Inputs of C into soluble and nonsoluble soil-C pools from plants could also be included, rendering them dynamic. A dynamic model will greatly increase computational demands, but this should not be a major impediment once the value of the architecture of the model is demonstrated. The importance of intermittent substrate limitation would likely increase in more complex and dynamic model structures.

The model currently represents the effects of wetting events only as it eliminates a constraint on diffusion of soluble substrates, but we also know that wetting events cause transient increases in soluble-C substrate concentrations resulting from microbial biomass that died or exudates that accumulated during dry periods (Birch, 1958; Kieft *et al.*, 1987). Failure to simulate the full range of observed soil respiration rates, and especially those associated with wetting events (Savage *et al.*, 2009), is largely related to this omission in the DAMM model structure, and it may partially explain the poor model fit for the wetting event on DOY 199, which was preceded by several days without rain. However, the DAMM model is designed to be able to integrate a module that simulates processes of releases of new soluble-C following wetting events, allowing released substrates to contribute to those that diffuse to the enzymatic reaction site.

Just as early attempts to simulate photosynthesis in dynamic vegetation models relied on the concept of a 'big leaf' to parsimoniously represent the combined photosynthetic apparatus of a landscape, the DAMM model currently simulates what might be called a 'big microsite' where all of the microbial respiratory enzymatic activity occurs in the soil. The calibrated parameters for the field data in the present version of the model, which simulates only one soluble substrate type, represent an effective mean value for all enzymatic activity that contributed to measured soil respiration at the study site. These values for Ea_{S_x}, a_{S_x}, and kM_{S_x} for the field data differ somewhat from those for the laboratory assays of two specific enzymes, but the laboratory assays were intended only to test model structure, and not to parameterize the model for other applications. As stated in the methods section, however, Eqn (1) could be employed any number of times in a more complex model, representing a different substrate-enzyme complex (S_x, S_y, S_z, …) in each use of the equation. This approach would be justified if we had information about each substrate–enzyme complex *in situ* that distinguished it from others, such as a distinctly different Ea_{S_x}, kM_{S_x}, or rate of substrate supply. An intermediate approach would be to use one equation to represent each family of substrates and enzymes with similar behaviors. For example, two or three families of substrates representing different levels of chemical recalcitrance, and hence different levels of activation energy and intrinsic temperature sensitivity (Davidson & Janssens, 2006), could be represented in the model to explore the importance of variations in activation energy values in different climate and substrate supply scenarios.

Soil is known for its extreme spatial heterogeneity and for the importance of processes occurring in diverse microsites within the soil. In its current form, diffusion of substrates is represented by simple functions [Eqns (4)–(6)] that effectively assume a mean diffusional distance to the microsites of enzymatic activity. A more complex two- or three-dimensional representation of the distribution of reactive sites and sources of substrates could be developed, or probability distribution functions of diffusional distances could be applied to the existing structure. This would also permit substitution of the current dimensionless diffusion coefficients with coefficients consistent with mathematical expressions of Fick's Law.

Microbial biomass, community structure, enzyme production, and enzyme properties are dynamic (Bradford *et al.*, 2010). The current DAMM structure includes parameters that can serve as simple proxies for this temporal and spatial variation in microbial dynamics. We have shown that the best fits for Ea_{S_x} and kM_{S_x} may vary seasonally, suggesting seasonal variation in the properties of the dominant enzymes

of heterotrophic respiration. In addition, seasonal variation in the best fit for the pre-exponent factor (a_{S_x}) of the Arrhenius equation for $V_{\max_{S_x}}$ [Eqn (2)], suggests that the enzymatic capacity may change seasonally, which may reflect variation in either microbial biomass and/or enzyme production. The higher a_{S_x} value calibrated for late spring and early summer, relative to other seasons (Table 4), would be consistent with a seasonal peak in enzyme capacity. At present, however, we have insufficient information to speculate on which, if any, of the seasonally variable model fits shown in Table 4 represents real variation in enzymatic capacity or properties. More complex model modules of microbial dynamics, such as those of Schimel & Weintraub (2003) or Allison *et al*. (2010) could link to DAMM, providing estimates of enzyme capacity and characteristics based on functions of microbial growth and enzyme production and constrained by related measurements.

The DAMM model is not meant as a full-fledged soil-C cycling model. Rather, it presents a mechanistic representation of how Arrhenius and Michaelis–Menten kinetics interact at the reactive sites of enzymes, leading to the production of CO_2 from metabolism of soluble-C substrates and/or substrates made soluble through depolymerization by soluble extracellular enzymes. It could serve as a core module that is informed by other modules regarding supply of soluble-C substrates and microbial dynamics. Most importantly, it presents a way forward from purely empirical representation of temperature and moisture responses and simulates integration of intrinsically temperature-sensitive enzymatic processes with equally important constraints of substrate supply.

Acknowledgements

This research was supported by the Northeastern Regional Center of the National Institute for Climatic Change Research, Grant No. DE-FC02-06ER64157.

References

Allison SD, Wallenstein MD, Bradford MA (2010) Soil-carbon response to warming dependent on microbial physiology. *Nature Geoscience*, **3**, 336–340.

Bengtson P, Bengtsson G (2007) Rapid turnover of DOC in temperate forests accounts for increased CO_2 production at elevated temperatures. *Ecology Letters*, **10**, 783–790.

Berry JA, Raison JK (1981) Responses of macrophytes to temperature. In: *Physiological Plant Ecology I. Responses to the Physical Environment* (ed. Lange OL), pp. 277–388. Springer-Verlag, Berlin.

Birch HF (1958) The effect of soil drying on humus decomposition and nitrogen availability. *Plant and Soil*, **10**, 9–32.

Bond-Lamberty B, Thomson A (2010) Temperature-associated increases in the global soil respiration record. *Nature*, **464**, 579–583.

Bradford MA, Watts BW, Davies CA (2010) Thermal adaptation of heterotrophic soil respiration in laboratory microcosms. *Global Change Biology*, **16**, 1576–1588.

Burnham KP, Anderson DR (2002) *Model Selection and Multi-Model Inference* (3rd edn). Springer, New York.

Conant RT, Ryan MG, Ågren GI *et al*. (2011) Temperature and soil organic matter decomposition rates – synthesis of current knowledge and a way forward. *Global Change Biology*, **17**, 3392–3404.

Davidson EA, Janssens I (2006) Temperature sensitivity of soil carbon decomposition and feedbacks to climate change. *Nature*, **440**, 165–173.

Davidson EA, Trumbore SE (1995) Gas diffusivity and production of CO_2 in deep soils of the eastern Amazon. *Tellus*, **47B**, 550–565.

Davidson EA, Belk E, Boone RD (1998) Soil water content and temperature as independent or confounded factors controlling soil respiration in a temperate mixed hardwood forest. *Global Change Biology*, **4**, 217–227.

Davidson EA, Verchot LV, Cattânio JH, Ackerman IL, Carvalho JEM (2000) Effects of soil water content on soil respiration in forests and cattle pastures of eastern Amazonia. *Biogeochemistry*, **48**, 53–69.

Davidson EA, Janssens IA, Luo Y (2006a) On the variability of respiration in terrestrial ecosystems: moving beyond Q10. *Global Change Biology*, **12**, 154–164.

Davidson EA, Savage K, Trumbore SE, Borken W (2006b) Vertical partitioning of CO_2 production within a temperate forest soil. *Global Change Biology*, **12**, 944–956.

Doran JW, Mielke IN, Power JF (1991) *Microbial activity as regulated by soil water-filled pore space*. Ecology of Soil Microorganism in the Microhabital Environments. Transactions of the 14th International Congress of Soil Sci. Symposium III-3, pp. 94–99, Kyoto, Japan.

Gaudinski JB, Trumbore SE, Davidson E (2000) Soil carbon cycling in a temperate forest: radiocarbon-based estimates of residence times, sequestration rates and partitioning of fluxes. *Biogeochemistry*, **51**, 33–69.

Hochachka PW, Somero GN (2002) *Biochemical Adaptation: Mechanism and Process in Physiological Evolution*. Oxford University Press, New York.

Kieft TL, Soroker E, Firestone MK (1987) Microbial biomass response to a rapid increase in water potential when dry soil is wetted. *Soil Biology Biochemistry*, **19**, 119–126.

Kirschbaum MUF (2010) The temperature dependence of organic matter decomposition: seasonal temperature variations turn a sharp short-term temperature response into a more moderate annually averaged response. *Global Change Biology*, **16**, 2117–2129.

Linn DM, Doran JW (1984) Effect of water-filled pore space on carbon dioxide and nitrous oxide production in tilled and nontilled soils. *Soil Science Society of America Journal*, **48**, 1267–1272.

Lloyd J, Taylor JA (1994) On the temperature dependence of soil respiration. *Functional Ecology*, **8**, 315–323.

Lonhienne T, Zoidakis J, Vorgias CE, Feller G, Gerday C, Bouriotis V (2001) Modular structure, local flexibility and cold-activity of a novel chitobiase from a psychrophilic antarctic bacterium. *Journal of Molecular Biology*, **310**, 291–297.

Magill AH, Aber JD, Berntson GM, McDowell WH, Nadelhoffer KJ, Melillo JM, Steudler P (2000) Long-term nitrogen additions and nitrogen saturation in two temperate forests. *Ecosystems*, **3**, 238–253.

Millington RJ (1959) Gas diffusion in porous media. *Science*, **130**, 100–102.

Papendick RI, Campbell GS (1981) Theory and Measurement of Water Potential. In: *Water Potential Relations in Soil Microbiology* (eds Parr JF, Gardner WR, Elliot LF), pp. 1–22. Soil Science Society of America Special Publications No. 9, Madison, WI.

R Development Core Team (2011) *R: A Language and Environment for Statistical Computing*. R Foundation for Statistical Computing, Vienna, Austria. ISBN 3-900051-07-0. Available at: http://www.R-project.org/ (accessed February 2011).

Ryan MG, Law BE (2005) Interpreting, measuring, and modeling soil respiration. *Biogeochemistry*, **73**, 3–27.

Saiya-Cork KR, Sinsabaugh RL, Zak DR (2002) Effects of long term nitrogen deposition on extracellular enzyme activity in an Acer saccharum forest soil. *Soil Biology and Biochemistry*, **34**, 1309–1315.

Savage K, Davidson EA (2003) A comparison of manual and automated systems for soil CO2 flux measurements: tradeoffs between spatial and temporal resolution. *Journal of Experimental Botany*, **54**, 891–899.

Savage K, Davidson EA, Richardson AD (2008) A conceptual and practical approach to data quality and analysis procedures for high frequency soil respiration measurements. *Functional Ecology*, **22**, 1000–1007, doi: 10.1111/j.1365-2435.2008.01414.x.

Savage KE, Davidson EA (2001) Interannual variation in soil respiration in two New England forests. *Global Biogeochemical Cycles*, **15**, 337–350.

Savage KE, Davidson EA, Richardson A, Hollinger DY (2009) Three scales of temporal resolution from automated soil respiration. *Agricultural and Forest Meterology*, **149**, 2012–2021.

Schimel JP, Weintraub MN (2003) The implications of exoenzyme activity on microbial carbon and nitrogen limitation in soil: a theoretical model. *Soil Biology and Biochemistry*, **35**, 549–556.

Sierra CA (2011) Temperature sensitivity of organic matter decomposition in the Arrhenius equation: some theoretical considerations. *Biogeochemistry*, doi: 10.1007/s10533-10011-19596-10539.

Skopp J, Jawson MD, Doran JW (1990) Steady-state aerobic microbial activity as a function of soil water content. *Soil Science Society of America Journal*, **54**, 1619–1625.

Šnajdr J, Valaskova V, Merhautova V, Herinokova J, Cajthaml T, Baldrian P (2008) Spatial variability of enzyme activities and microbial biomass in the upper layers of Quercus petraea forest soil. *Soil Biology and Biochemistry*, **40**, 2068–2075.

Subke JA, Bahn M (2010) On the 'temperature sensitivity' of soil respiration: can we use the immeasurable to predict the unknown? *Soil Biology and Biochemistry*, **42**, 1653–1656.

Tarnocai C, Canadell JG, Schuur EAG, Kuhry P, Mazhitova G, Zimov S (2009) Soil organic carbon pools in the northern circumpolar permafrost region. *Global Biogeochemical Cycles*, **23**, doi: 10.1029/2008GB003327.

Valásková V, Šnajdr J, Bittner B, Cajthaml T, Erhautová V, Hofrichter M, Baldrian P (2007) Production of lignocellulose-degrading enzymes and degradation of leaf litter by saprotrophic basidiomycetes isolated from a Quercus petraea forest. *Soil Biology and Biochemistry*, **39**, 2651–2660.

von Lützow M, Kögel-Knabner I (2009) Temperature sensitivity of soil organic matter decomposition—what do we know. *Biology and Fertility of Soils*, **46**, 1–15.

Supporting Information

Additional Supporting Information may be found in the online version of this article:

Appendix S1. Dual Arrhenius and Michaelis–Menten (DAMM) kinetics model function coded for the statistical package R. The following code corresponds to the configuration of the DAMM model used for modeling the field data described in the text. Arguments to the model function are the calibrated parameters, soil temperature (soil *T*, °C) and soil moisture (soil *M*, %). The fixed parameter values shown here are specific to the field data used in this study.

Please note: Wiley-Blackwell are not responsible for the content or functionality of any supporting materials supplied by the authors. Any queries (other than missing material) should be directed to the corresponding author for the article.